Journal of
Marine Science and Engineering

MDPI

Article

Power Prediction Method for Ships Using Data Regression Models

Yoo-Chul Kim *, Kwang-Soo Kim, Seongmo Yeon, Young-Yeon Lee, Gun-Do Kim and Myoungsoo Kim

Korea Research Institute of Ships and Ocean Engineering (KRISO), Yuseongdae-ro 1312beon-gil, Yuseong-gu, Daejeon 34103, Republic of Korea; ksookim@kriso.re.kr (K.-S.K.); seongmo.yeon@kriso.re.kr (S.Y.); yylee@kriso.re.kr (Y.-Y.L.); gdkim@kriso.re.kr (G.-D.K.); mskim@kriso.re.kr (M.K.)

* Correspondence: kimyc@kriso.re.kr

Abstract: This study proposes machine learning-based prediction models to estimate hull form performance. The developed models can predict the residuary resistance coefficient (C_R), wake fraction (w_{TM}), and thrust deduction fraction (t). The multi-layer perceptron and convolutional neural network models, wherein the hull shape was considered as images, were evaluated. A prediction model for the open-water characteristics of the propeller was also generated. The experimental data used in the learning process were obtained from model test results conducted in the Korea Research Institute of Ships and Ocean Engineering towing tank. The prediction results of the proposed models showed good agreement with the model test values. According to the ITTC procedures, the service speed and shaft revolution speed of a ship can be extrapolated from the values obtained from the predictive models. The proposed models demonstrated sufficient accuracy when applied to the sample hull forms based on data not used for training. Thus, they can be implemented in the preliminary design phase of hull forms.

Keywords: machine learning; convolutional neural network; multi-layer perceptron; resistance; propulsion; power prediction

Citation: Kim, Y.-C.; Kim, K.-S.; Yeon, S.; Lee, Y.-Y.; Kim, G.-D.; Kim, M. Power Prediction Method for Ships Using Data Regression Models. *J. Mar. Sci. Eng.* **2023**, *11*, 1961. https://doi.org/10.3390/jmse11101961

Academic Editors: Panagiotis D. Kaklis, Konstantinos Kostas and Shahroz Khan

Received: 25 August 2023
Revised: 4 October 2023
Accepted: 4 October 2023
Published: 11 October 2023

1. Introduction

Recent environmental regulations, such as the energy efficiency design index of the International Maritime Organization, demand the design of hydrodynamically efficient hull forms. In particular, a crucial indicator of hydrodynamic efficiency is the power required in calm waters, obtained from the resistance and propulsion characteristics and their relationship with the propeller open water (POW) characteristics. Therefore, predicting the performance characteristics, such as residuary resistance coefficient (C_R), wake fraction (w_{TM}), thrust deduction fraction (t), and POW characteristics, is essential in the design stage. Computational fluid dynamics (CFD), model tests, and data-driven methods have been used to estimate these coefficients. Generally, model tests is used in the final design stage of a hull form to accurately confirm the performance of the hull; however, these tests require considerable cost and time. Recent advances in computing power have led to CFD being actively used in the design review stage for optimal hull form alternatives. However, implementing CFD is still slow because calculating multiple alternatives for optimization requires days or weeks and is challenging to conduct without large computational resources. In contrast, data-driven prediction models such as series charts, regression equations, and machine learning models can be applied for hydrodynamic design (e.g., the determination of the main parameters of hull forms) in the preliminary design stage, where the low accuracy compared to that of CFD or model tests is not a significant aspect, because they provide a fast feedback. In particular, the rapid advances in data analysis technologies, such as deep neural networks (DNNs) and convolutional neural networks (CNNs), have improved traditional regression methods. Thus, machine learning models considering hull shape itself have the potential to assist CFD in the hull form optimization process, although this solution may not be a complete alternative.

The seminal study regarding the data-driven prediction of the performance characteristics of hull forms was the standard series of experiments by Taylor [1] in the 1930s. Subsequently, prediction methods based on experiments reanalyzing the Taylor series chart have been introduced, such as the Gertler chart [2] and the Netherland ship model basin (NSMB) Lap chart [3]. Guldhammer and Harvald [4] predicted the effective power using a diagram developed by arranging the towing test results in groups according to the length–displacement ratio ($\frac{L}{\nabla^{1/3}}$) and prismatic coefficient of the model ($\varphi = \frac{\nabla}{LBT\beta}$, where β is the midship section area coefficient). Holtrop and Mennen analyzed the model test results and derived regression-based formulations for resistance and propulsion characteristics from 1978 to 1984 [5–7]; these formulations are currently used to determine the main parameters with some modified coefficients in numerous shipyards. Kim et al. [8] defined several geometric variables of the hull form and developed regression equations for the residuary resistance coefficient. The equations were developed by analyzing the model test results of the Korea Research Institute of Ships and Ocean Engineering (KRISO). Studies on applying machine learning schemes for performance prediction have also been introduced. In particular, Kim et al. [9] expanded the regression model in [8] and applied it to an ensemble model. Cho et al. [10] generated 1263 hull forms by modifying the KVLCC2 hull form and learned the three-dimensional (3D) coordinates of the cross-sections to fit the resistance results computed from Holtrop and Mennen's formula. They built a DNN model. Bertram and Mesbahi [11] presented an artificial neural network (ANN) model to predict calm sea resistance and power of fast monohulls using principal dimensions, whereas Couser et al. [12] applied a neural network to interpolate the experimental results of a catamaran series. Yang et al. [13] predicted the resistance of a 13,500 TEU container carrier under several draft conditions using a radial basis function neural network (RBFNN). Moreover, Cepowski [14] introduced an ANN model to estimate the added resistance in waves using the principal dimensions of a ship, and Liu and Papanikolaou developed semi-empirical equations for added resistance estimation under various wave conditions [15–17]. Martić et al. [18,19] applied the ANN for the evaluation of added resistance of container ships successfully. Their model was based on the LM (Levenberg–Marquardt) learning algorithm with BR (Bayesian regularization). The prediction of the residuary resistance coefficient of a trimaran model using ANN with the transverse and longitudinal positions of the side hulls, the longitudinal center of buoyancy, and the Froude number was introduced by Yidiz [20]. A study on flow field estimation conducted by Ichinose and Taniguchi [21] proposed a curved surface representation method suitable for a CNN to predict the nominal wakefield. Optimizing hull shapes using surrogate models [22–24] has also been introduced. However, some regression equations rely on outdated data, and the accessibility to modern hull forms and model test data is limited.

In this study, the power prediction of a ship using only data regression models was introduced. The relatively modern hull forms and the model test results were analyzed. The regression model focused on the CNN model; however, MLP (Multi-Layer Perceptron) model was also provided in case details of the hull geometry are not available. A hull geometry representation method relying on images to apply CNN to predict the ship hydrodynamic characteristics is proposed. In this regard, the cross-sectional shape was converted into an image with one channel and then used as an input for the prediction models. This approach has the following advantages. Firstly, three dimensional geometric features can be captured. Most of the previous studies using several variables as inputs are limited in this aspect. The second is that the segmentation of ship type is not necessary because it is already included in the hull geometry. The third is that this method, considering hull geometry itself, can be used as a surrogate model in the hull form optimization process. The last is that this approach combined with generative models such as VAE (Variational Auto Encoder) or GAN (Generative Adversarial Networks) can be used in hull form generation.

This paper is organized as follows. Section 2 shows how to construct regression models and train datasets. In Section 3, learning results of each prediction model for resistance and propulsion characteristics are shown. Section 4 presents the power prediction process using the present network models and the results of the case studies, which are followed by the conclusions and the future research works.

2. Methods

The final goal of this study is to estimate the required power of a ship using only regression models. The MLP model estimates the resistance and propulsion characteristics from the principal dimensions of a ship, whereas the CNN model needs the additional input of hull geometry. Hull geometry representation for the CNN model and the method for constructing each regression model are described in this section. Section 2.1 provides the method to convert the hull geometry into images. The structure of the prediction models is explained in Section 2.2. The details of the training data and the set-up of the network model are provided in Section 2.3.

2.1. Hull Geometry Representation

The resistance and propulsion characteristics of a hull form are primarily related to its geometry. Wave-making resistance is strongly related to the fore-body geometry of a hull. Moreover, the after-body geometry affects the pressure resistance and propulsion characteristics. CNN is widely used in image data recognition. Therefore, a CNN able to capture the changing patterns of the hull geometry may be effective if the hull geometry can be converted into images. In this study, an $N \times N$ pixel image was generated corresponding to a cross-section of the hull form. In general, a hull surface consists of a longitudinal array of two-dimensional cross-sectional information (y, z); the coordinates have different values depending on the size of the ship. In this study, the cross-section geometry was non-dimensionalized in terms of half breadth and draft to consider only geometric characteristics. The maximum height of the cross-section was set to 1.1 times the draft. First, the cross-section was converted to a binary pixel image where the hull surface was set to 1 and the other area to 0, as shown in Figure 1. Bresenham's line algorithm [25] was used to obtain the pixels between two points on the hull surface. However, when binary pixel images were used, precise results could not be expected because of the insufficient information in the image. Therefore, a signed distance function (SDF) was adopted to add additional information to the images. The SDF is the orthogonal distance of a given point to the boundary of the hull and is determined by whether the given point is in the interior of the hull. The function not only distinguishes the object's boundary but also expresses the region away from the boundary. Guo and Iorio [26] successfully applied SDF to create a surrogate model for CFD. The pixel value is defined using Equation (1). The boundary of the hull is expressed as 0; the inside has a positive value, and the outside has a negative value. The minimum distance from the boundary was stored as a pixel value, and the distance was normalized by the diagonal length of the image. Figure 2 illustrates the image representation using the SDF.

$$D(i,j) = min_{(i',j' \in Z)} \left| (i,j) - (i',j') \right| sign(f(i,j)) \quad (1)$$

2.2. Model Construction

2.2.1. CNN Model

The developed prediction model based on the cross-sectional images is introduced in this section. The principal dimensions of the ship are used as additional inputs to the hull form images because the cross-sectional coordinates are non-dimensionalized. Therefore, the model has multiple-inputs and a single-output structure. One of the inputs for the hull-form geometry is (3D) voxel data, where two-dimensional (2D) cross-section images are stacked in the longitudinal direction. If the cross-sectional image is created as $[N \times N]$, and M stations are used for hull form definition, the input dimensions are $[M \times N \times N]$.

Moreover, the input data for the hull geometry are passed through a series of 3D CNN layers to detect the changing sectional shape patterns. The main dimensions of the hull form are also used as inputs. These hull form dimensions can be combined with the latent vector obtained from the convolution layers and passed through several MLP neural networks before the output layer, as illustrated in Figure 3. The final model is generated by learning in a direction of reducing the difference between the predicted and ground truth values (model test result) to a particular target value. Some schemes for preventing overfitting, such as dropout and regularization, can be applied.

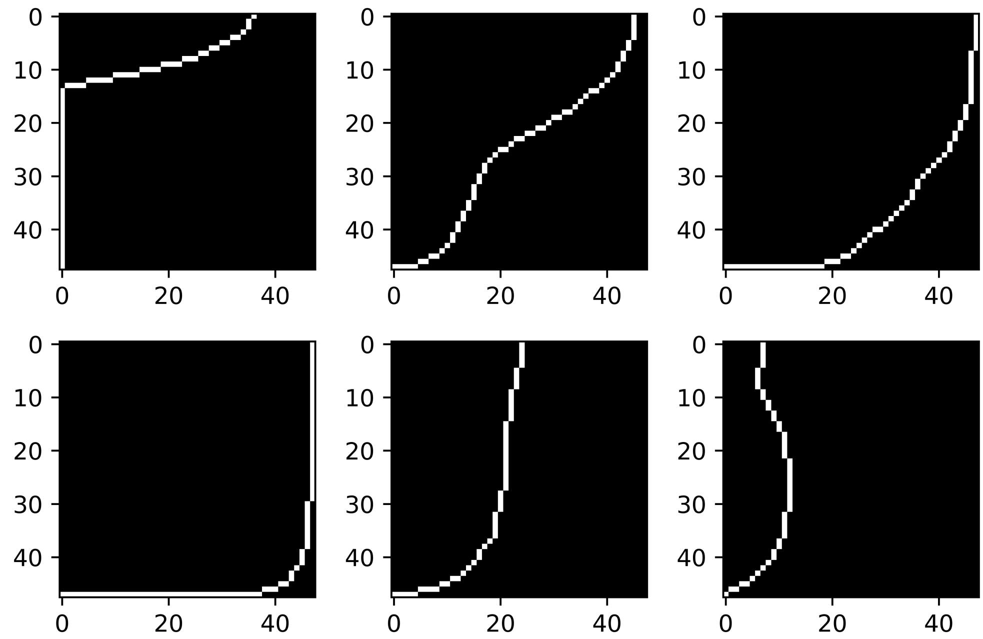

Figure 1. Binary pixel image representation.

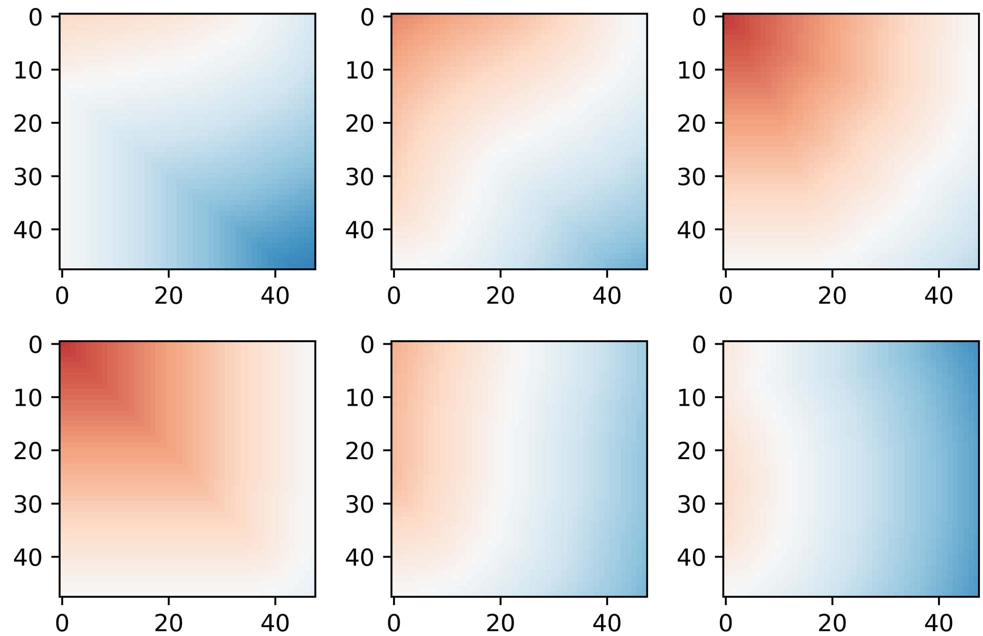

Figure 2. SDF pixel image representation.

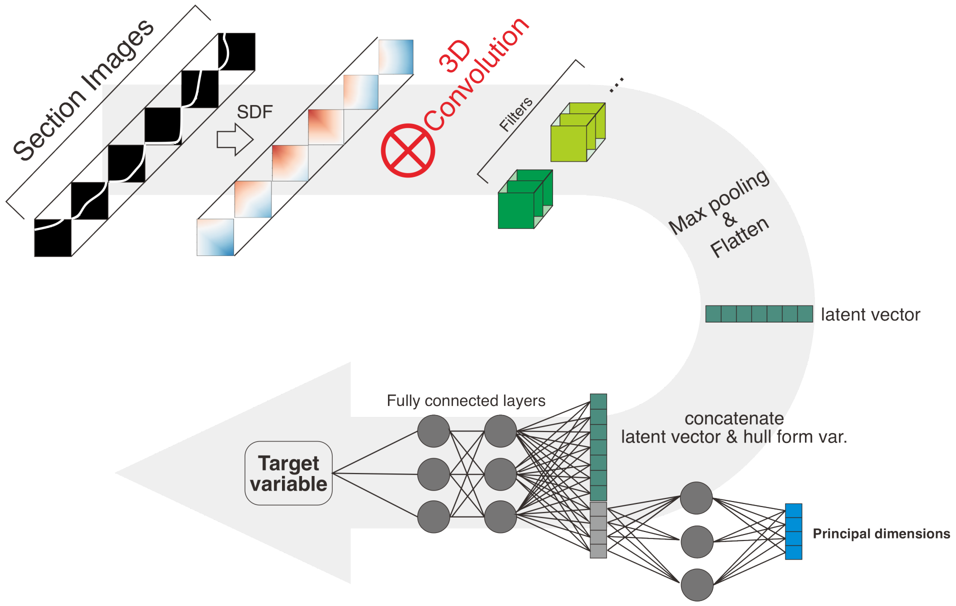

Figure 3. Overall concept of the CNN model.

A block coefficient (C_B) prediction model was constructed and tested to validate the proposed approach considering the cross-sectional shapes of the hull. Because C_B is defined by the displacement volume ratio to LBT, this coefficient can be obtained by integrating the dimensionless cross sections in the longitudinal direction. Hence, this model does not require the principal dimensions as the second input. In this study, 80% of the hull form data were used for training, and the rest were used for model assessment. Three convolution layers and max-pooling were applied, and a fully connected layer with 256 nodes was connected to C_B. Figure 4 presents the C_B prediction results obtained using this model. R^2 for the test data was 0.996, indicating excellent performance. From this case, it can be indirectly confirmed that the CNN model using image-converted cross-sections can capture the geometric characteristics of the hull form.

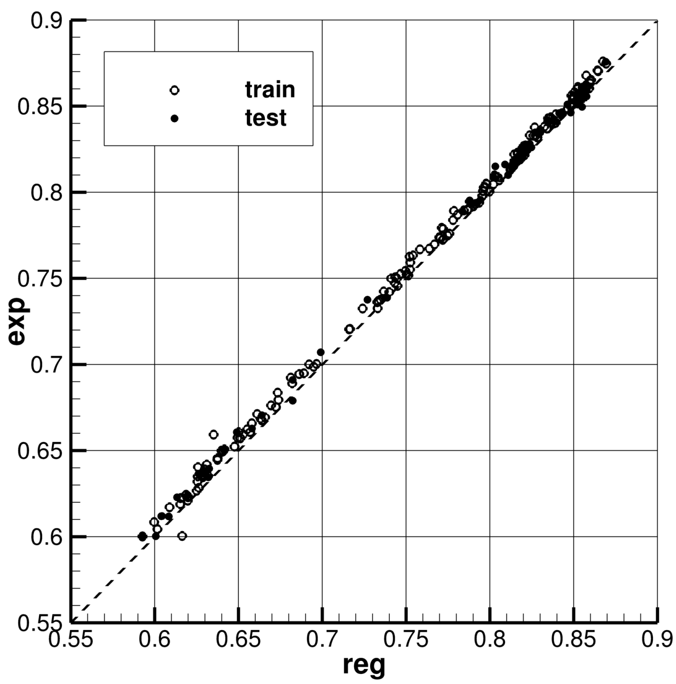

Figure 4. C_B predicted by the CNN model.

2.2.2. MLP Model

A model that uses only the principal dimensions of the ship is required if the cross-sectional shapes are not available. In this model, the input values are connected to the output through several fully connected layers, as shown in Figure 5. Each fully connected layer has multiple nodes with weight and bias. These values can be adjusted to reduce output errors during the learning process. This structure of the MLP model was also used in the prediction model for the POW characteristics.

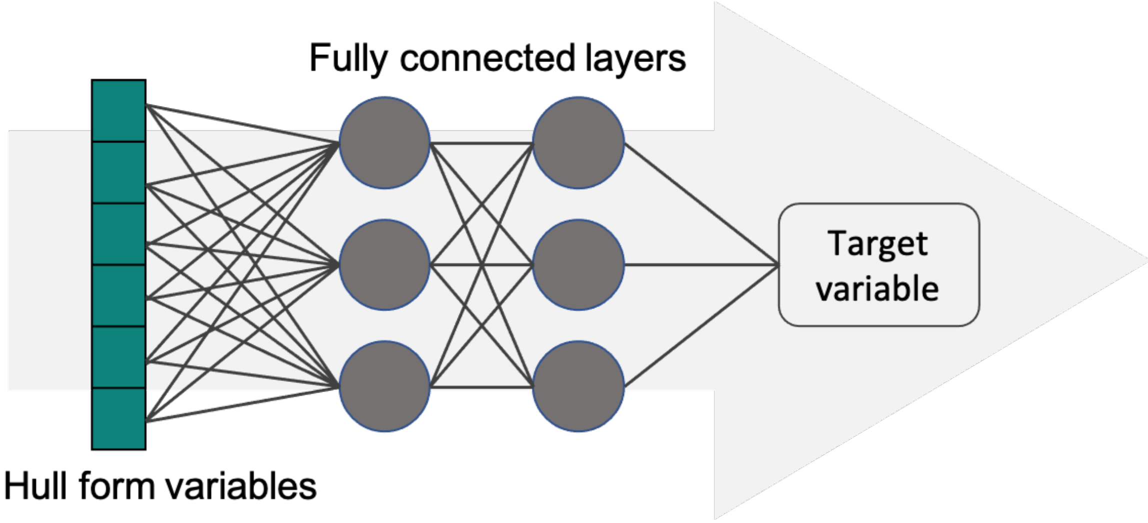

Figure 5. Overall concept of MLP model.

2.3. Training Data

Towing test results for resistance and self-propulsion of 217 ships were analyzed in this study. All the experiments were conducted at Korea Research Institute of Ships and Ocean Engineering (KRISO). The data included that of single-shaft commercial ships (bulk carriers, tankers, container carriers, and gas carriers); only the design draft conditions were considered. The outliers and missing values were excluded from the analysis. Figure 6 shows the distribution of the selected hull form variables. Length of the ships varies from 100 m to 400 m. To decrease the possibility of overfitting, holdout cross-validation and k-fold validation for hyperparameter tuning were used, as shown in Figure 7. The final regression models were created by using the training data and the validation data sets, and the models were evaluated by applying them to the test data set. The data for training were set to 80% on a hull basis, and the remaining data (20%) were used for testing. The input variables of the principal dimensions and output values were normalized using the mean values and standard deviations. Segmentation by ship type was not applied because the cross-sectional shapes reflected the characteristics of each ship type. The network weights were initialized by He uniform [27] and updated by RMSprop [28] to minimize the mean squared error (MSE). The nonlinear activation function ReLU was used, and early stopping was employed to determine the optimum number of epochs. Batch normalization was not applied because this technique is typically employed with very deep neural networks and does not perform well with the present models. During the hyperparameter tuning step, the training dataset was divided into three folds, and the averaged validation score was computed to assess a hyperparameter set. The numbers of nodes and layers were determined using the grid search method, and the dropout rate and L2 regularization factor were determined using Bayesian optimization [29].

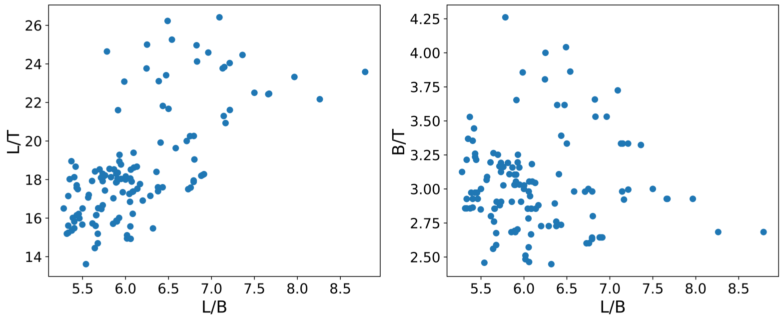

Figure 6. Hull form variable distributions.

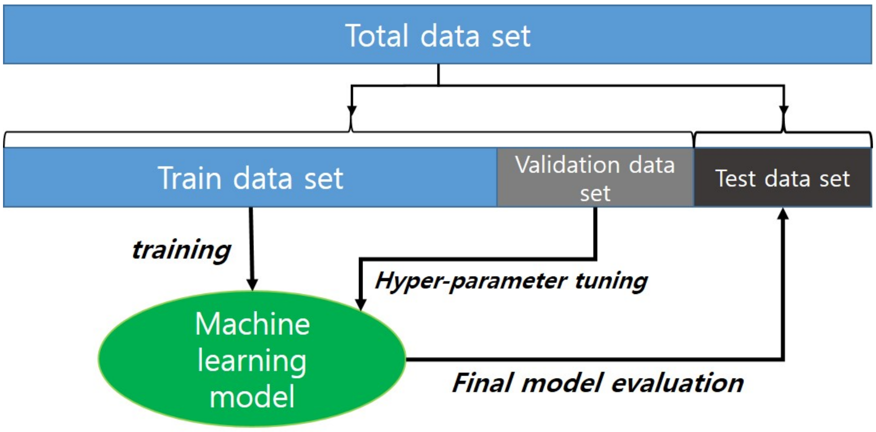

Figure 7. Holdout cross-validation.

3. Prediction Results Regarding the Ship Hydrodynamic Characteristics

As mentioned previously, the coefficients related to the resistance, self-propulsion, and propeller open-water characteristics should be predicted to compute the required power of a ship. Three prediction models were developed. One model was for the residuary resistance coefficient (C_R), another considered the wake fraction and thrust deduction fraction (w_{TM}, t), and the third focused on the POW characteristics (K_{TM} and K_{QM}).

3.1. Residuary Resistance Coefficient

3.1.1. CNN Model

The hull cross-sections for inputs were obtained from after-perpendicular (AP) to forward-perpendicular (FP); hence, information regarding the bulbous bow was needed. Therefore, length of the bulbous bow was used as the input for the principal dimensions. Moreover, the Froude number (Fr) was used because the speed of the ship is the most important factor affecting C_R. The total input values of the principal dimensions for C_R were selected as $\frac{L}{B}, \frac{L}{T}, \frac{B}{T}, \frac{L}{\nabla^{1/3}}, Fr, and \frac{L_{bulb}}{L}$. A total of 23 stations were used for the input of cross-sections, where the smallest interval was $0.025L$, and the largest was $0.1L$. The image size of a cross-section was 96×96, with a resolution of approximately 1%. The number of $Fr - C_R$ set was 2011.

The final model obtained from the hyperparameter tuning has [12-8-8] 3D convolution layers for the image sequence ($23 \times 96 \times 96$), [64] fully connected layers for the principal dimensions and [32-32] fully-connected layers for the concatenated data, as illustrated in Figure 8. The size of the convolution kernel was ($3 \times 3 \times 3$), and a stride with dimensions ($2 \times 2 \times 2$) was applied at the first convolution layer.

Figure 9 presents the results for $C_R \times 10^3$ predicted using the proposed CNN model. The hollow symbols indicate the training data results, and the solid symbols indicate those of the test data. The horizontal axis represents the predicted value from the regression model, and the vertical axis represents the ground truth (model test results). The coefficient of determination (R^2) for the training data was calculated as 0.985, while the R^2 for the test data was 0.928. A good correlation was confirmed between the estimated and ground-truth values. In contrast to calculating the errors for individual data, the error for one hull form was calculated by dividing the integrated value of the absolute error in the speed range by the integrated true value, as shown in Equation (2), because the error for one hull form in the speed range is also important. The average error of C_R for the entire dataset was 4.13%, and that of the total resistance of the model (R_{TM}) was 0.95%.

$$err_{ship}(\%) = \frac{\int_{Fr} \left| Val_{pred} - Val_{true} \right| dFr}{\int_{Fr} Val_{true} dFr} \times 100 \quad (2)$$

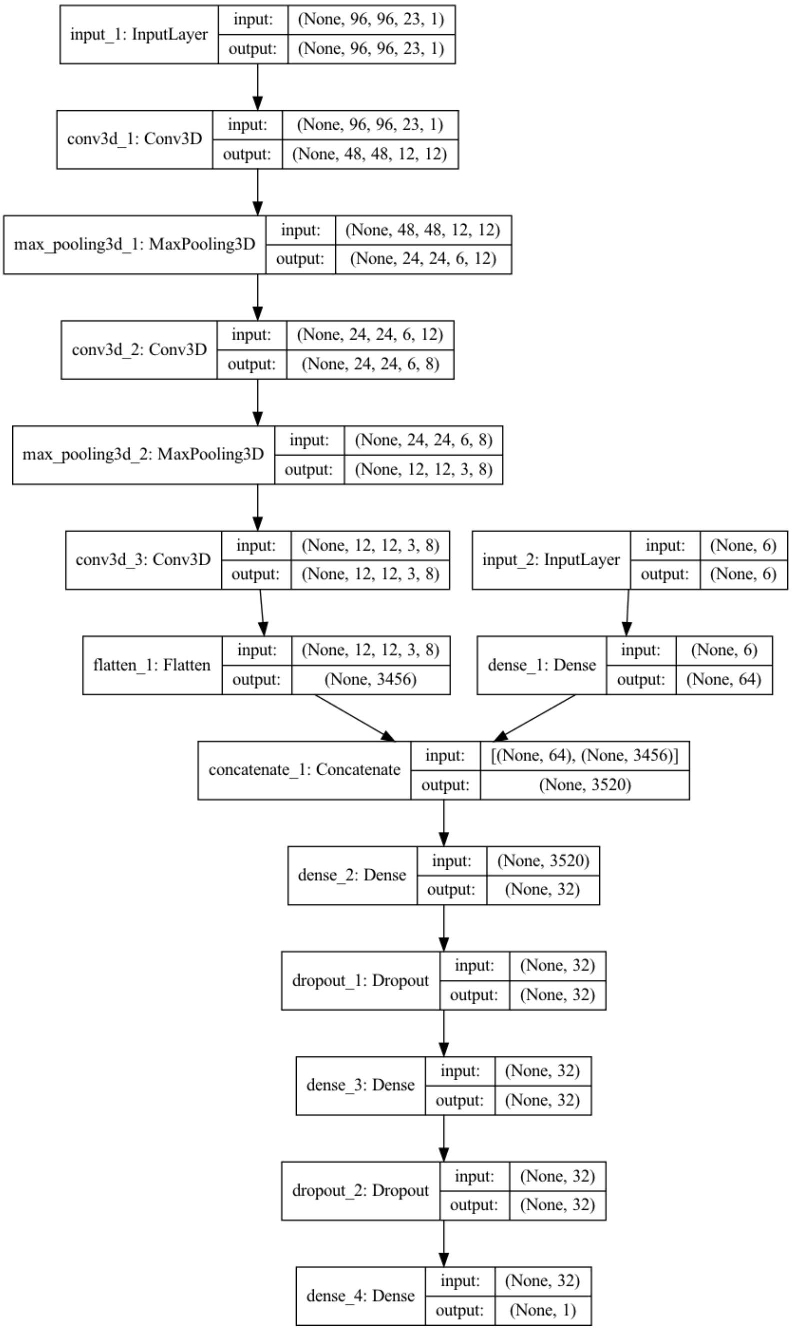

Figure 8. Structure of the CNN model for C_R.

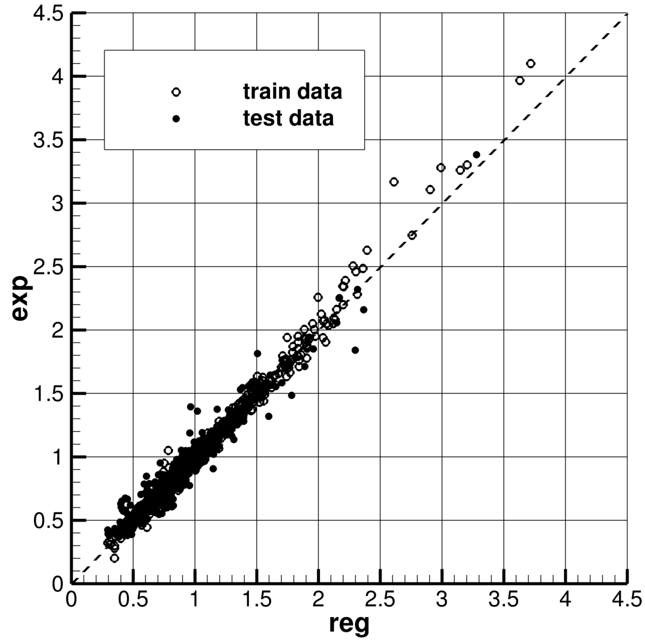

Figure 9. C_R predicted results from the CNN model.

3.1.2. MLP Model

In this model, only the principal dimensions were used as inputs (Figure 5). The selected dimensions were $\frac{L}{B}$, $\frac{L}{T}$, $\frac{B}{T}$, $\frac{L}{\nabla^{1/3}}$, Fr, $\frac{L_{bulb}}{L}$, and L_{CB}. L_{CB} was added to the inputs of the CNN model to consider the volume distribution of the hull. Three fully connected layers [128-64-32] were used. Figure 10 presents the predicted results. A larger deviation than the CNN model was confirmed. The R^2 values for the training and test data were 0.910 and 0.814, respectively. The average error of C_R was 8.69%, and that of R_{TM} was 1.97%. These errors are approximately two times that of the CNN model. However, it is confirmed that several principal dimensions largely determined the resistance characteristics of a hull form.

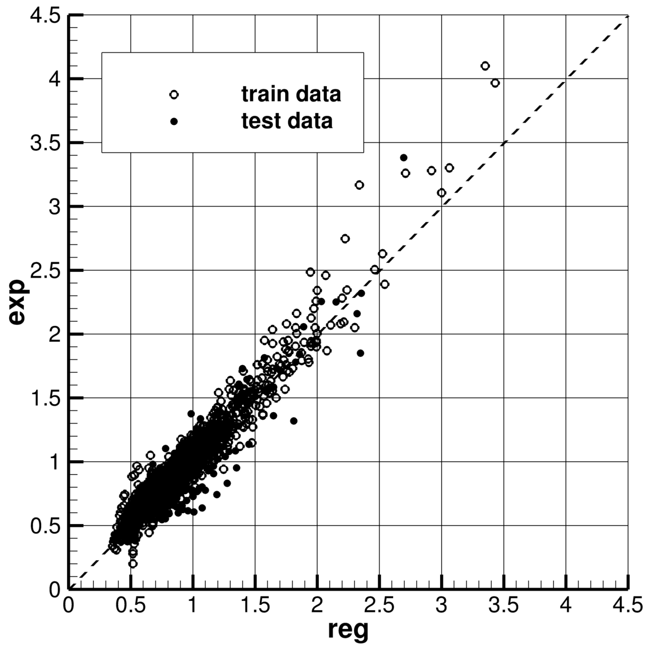

Figure 10. C_R predicted results from the MLP model.

3.2. Wake and Thrust Deduction Fractions

3.2.1. CNN Model

The model structure for the wake and thrust deduction fraction coefficients related to propulsion characteristics was essentially the same as that for the residuary resistance coefficient. However, assuming that the contribution of the frontal shape of the hull was small, only 12 afterbody cross-sections were used as the input in the analysis, and the length of bulbous bow was not considered as input of the principal dimensions. The block coefficients of the afterbody (C_{BA}) and the propeller diameter ($\frac{D_P}{T}$) were added instead. Figure 11 illustrates the structure of the model. The model had [8-8-4] 3D convolution layers and [64] fully-connected layers for the principal dimensions and [64-32] fully-connected layers for the concatenated data. The convolution kernel size and stride setting were the same as those in the C_R model. The output layer had a dimension of two for the wake fraction (w_{TM}) and thrust deduction fraction (t). Figure 12 shows the results. The R^2 values of the test data for w_{TM} and t were computed as 0.863 and 0.550, respectively. The average errors for all the data were 3.08% and 3.85% for each item. Some discrepancies were observed between the regression and true values for t. However, this error level is considered to be not excessive because t is used in terms of $1 - t$ when computing the required power of a ship.

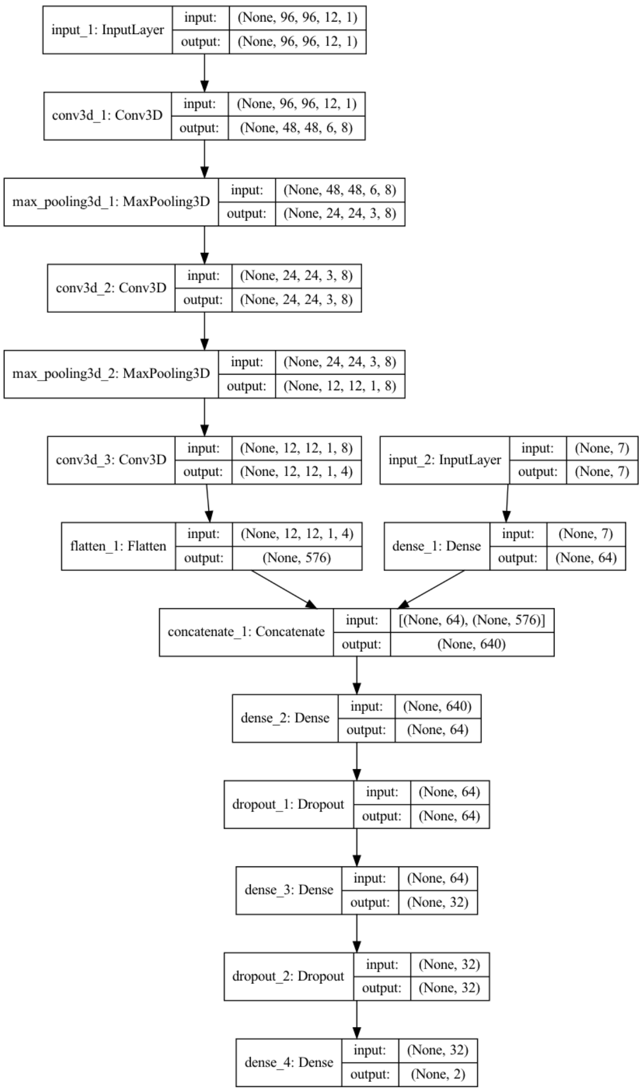

Figure 11. Structure of the CNN model for w_{TM} and t.

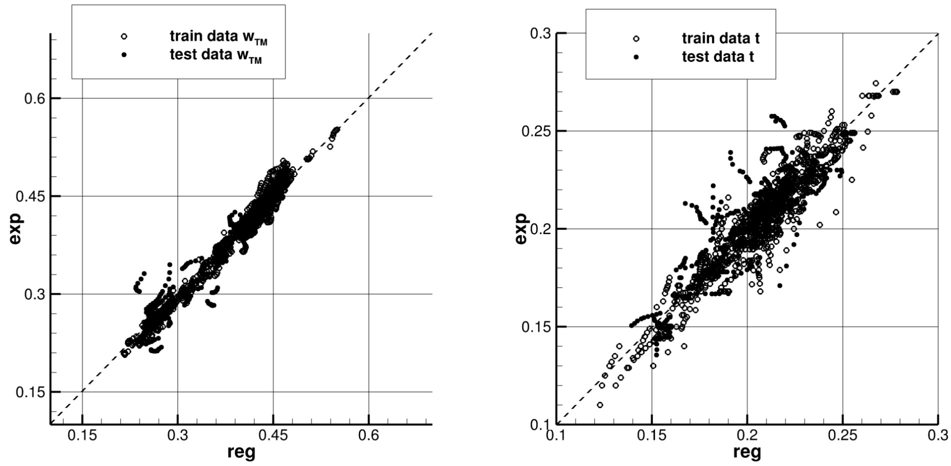

Figure 12. w_{TM} (**left**) and t (**right**) predicted results from the CNN model.

3.2.2. MLP Model

In this model, the same inputs for the principal dimensions as those used in the CNN model were used. Figure 13 presents the predicted results. No significant loss in accuracy of the MLP model was observed compared to the C_R case. The R^2 values of the test data for w_{TM} and t were computed as 0.748 and 0.409, respectively. The results confirmed that cross-sectional information could improve the prediction performance of the propulsion coefficients for the test data.

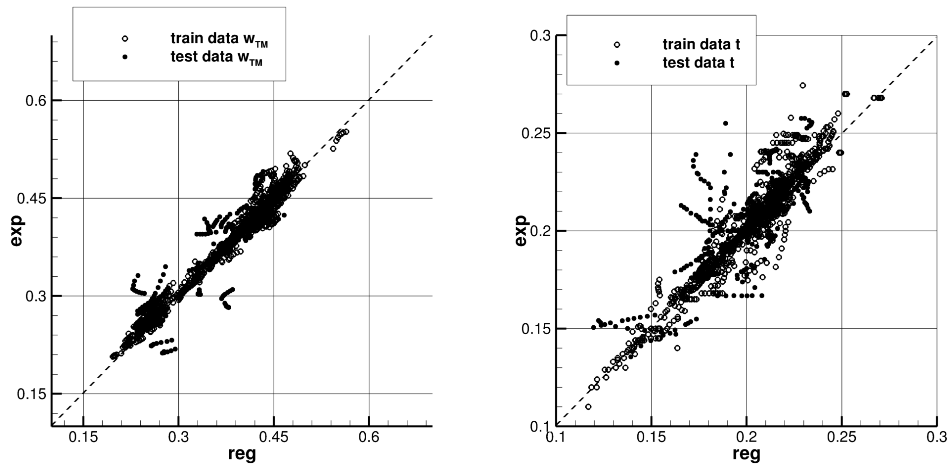

Figure 13. w_{TM} (**left**) and t (**right**) predicted results from the MLP model.

3.3. POW Characteristics

The Maritime Research Institute Netherlands (MARIN) B-series and the National Maritime Research Institute (NMRI) MAU series are widely used POW regression models. In this study, MLP models for predicting K_{TM} and K_{QM} were developed. Because the propeller has a relatively standard shape and its shape can be easily reproduced by a few key parameters, even a simple MLP model can show a precise prediction. In this study, only one fully connected layer was used. The POW results of 483 propellers were used for learning, and these propellers had only NACA and KH (KRISO-developed) section shapes. Fixed pitch propellers with seven blades or less and a hub ratio of less than 0.22 were used for the analysis. These types of propellers are generally used in commercial ships. The input variables were the advance ratio (J), number of blades (Z), expanded blade area ratio (a_E), pitch ratio at 0.7R ($p_{0.7R}$), and mean pitch ratio (p_{mean}). The number of nodes in the fully connected layers was 48. Outstanding results were confirmed, as shown in Figure 14. The R^2 of the test data for K_{TM} was 0.995, and for K_{QM} was 0.992. The average error, as defined in Equation (2), was approximately 3% for both coefficients. As the B-series regression showed an error of approximately 6% for the same data, improved prediction errors were obtained.

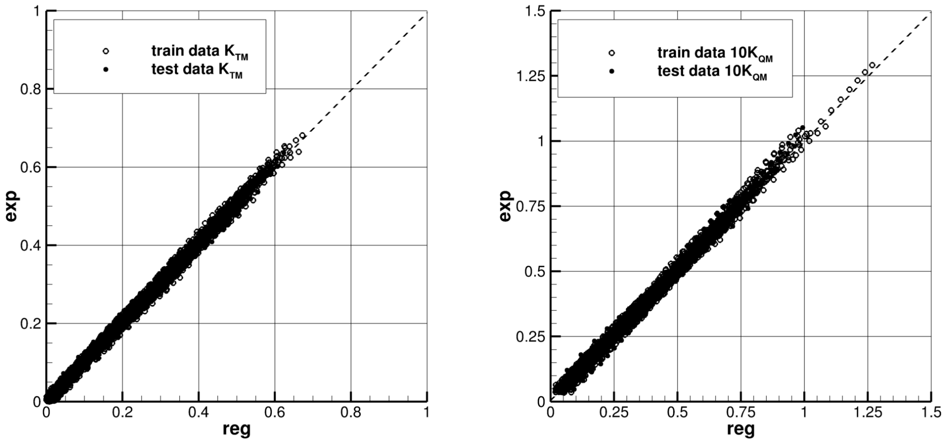

Figure 14. K_{TM} (**left**) and $10K_{QM}$ (**right**) predicted results from the MLP model.

3.4. Summary of the Final Models

Table 1 shows the summary of input variables and network layers for each regression model finally obtained by hyperparameter tuning.

Table 1. Model structures and input data.

	Residuary Resistance Coeff.		Wake & Thrust Deduction Fraction		POW Characteristics
	CNN	MLP	CNN	MLP	MLP
Hull geom.	23 stations w/ 96 × 96 image (23 × 96 × 96)	-	12 stations w/ 96 × 96 image (12 × 96 × 96)	-	-
Input var.	$\frac{L_{bulb}}{L}$	$\frac{L}{B}$, $\frac{B}{T}$, $\frac{L}{T}$, $\frac{L}{\nabla^{1/3}}$, Fr L_{CB}	C_{BA}, $\frac{D_P}{T}$	C_{BA}, $\frac{D_P}{T}$	J, Z, A_E $p_{0.7R}$, p_{mean}
CNN layer	[12-8-8] w/ kernel size 3	-	[8-8-4] w/ kernel size 3	-	-
MLP layer for input var.	[64]	[128-64 -32]	[64]	[128-64 -32]	[48]
MLP layer for concat.	[32-32]	-	[64-32]	-	-

4. Power Prediction

4.1. Performance Prediction Method

The coefficients of resistance, self-propulsion, and POW characteristics were estimated using the developed regression models. The power required by a full-scale ship can be calculated using an the ITTC 1978 performance prediction method based on two-dimensional extrapolation [30], as shown in Figure 15. Because the regression models estimate the performance coefficients at the model scale, extrapolation to the full scale was required. The two-dimensional extrapolation method was used in KRISO, as shown in Equation (3). The bilge keel area (S_{BK}) was assumed as 0.9% of the wetted surface area (S_{BH}). S_{BH} can be used as a known value or obtained from the regression result (Equation (4)). C_A can also be used as a known value or computed using a simple regression formula such as Equation (5). C_{FS} is the frictional resistance coefficient of the ship according to the ITTC-1957 model-ship correlation line, as shown in Equation (6), while C_{AA}, which denotes the air or wind resistance coefficient, can be obtained from Equation (7) using the projected area of the ship above the waterline to the transverse plane.

$$C_{TS} = \frac{S_{BH} + S_{BK}}{S_{BH}}[C_{FS} + C_A] + C_R + C_{AA} \tag{3}$$

$$S_{BH} = -0.00000017\nabla^2 + 0.131902474\nabla + 2307.018044 \tag{4}$$

$$C_A = 0.000008121L^2 - 0.005691L + 0.683357299 \tag{5}$$

$$C_{FS} = \frac{0.075}{(log_{10}Rn - 2)^2} \tag{6}$$

$$C_{AA} = 0.8\frac{\rho_A A_T}{\rho_S S_{BH}} \tag{7}$$

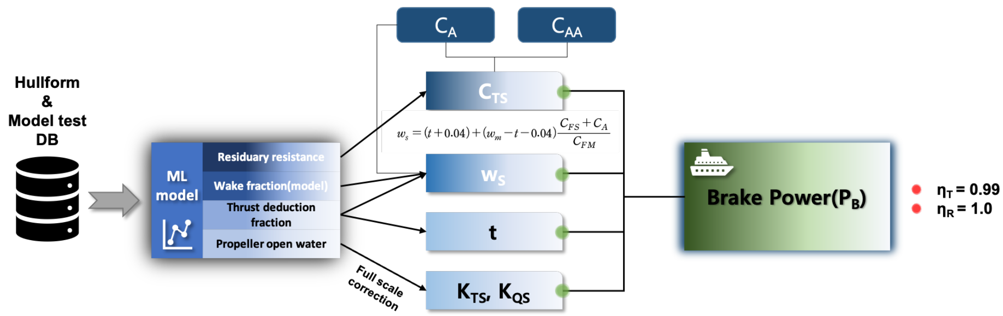

Figure 15. Overall concept of the power prediction for the full scale ship.

The wake fraction at full scale was extrapolated using the thrust deduction fraction and frictional resistance coefficients, as shown in Equation (8).

$$w_{TS} = (t + 0.04) + (w_{TM} - t - 0.04)\frac{C_{FS} + C_A}{C_{FM}} \tag{8}$$

The POW characteristics of full-scale propellers are generally obtained using the ITTC extrapolation method. However, following this approach requires detailed information on the propeller blade section shape. If we assumed that such detailed information is not available, it was simply converted to a 1% increase in K_T and a 1% decrease in K_Q of the model scale value in this study. The load of the full-scale propeller was computed as follows:

$$\left(\frac{K_T}{J^2}\right)_S = \frac{S_{BH}}{2D_P^2}\frac{C_{TS}}{(1-t)(1-w_{TS})^2}. \tag{9}$$

The advance ratio (J_{TS}) and torque coefficient (K_{QTS}) of the propeller can be obtained from the POW curve using the thrust coefficient identity. The brake power (P_B) can be computed using Equation (10), where the relative rotative efficiency (η_R) and the transmission efficiency (η_T) were assumed as 1.0 and 0.99, respectively. n_S represents the propeller frequency of the revolution at the self-propulsion point.

$$P_B = 2\pi\rho_S D_P^5 n_S^3 \frac{K_{QTS}}{\eta_R \eta_T} \cdot 10^{-3} \tag{10}$$

4.2. Case Study

This section presents the results of applying the regression models and power prediction process for four cases of commercial ships. In particular, the data of a 176 m bulk carrier, a 206.55 m container carrier, 165 m LPG carrier, and a 320 m tanker were selected from test data not used to develop the model. The main parameters and the input values of the ships are listed in Table 2. Figure 16 presents a comparison of the required power and service speed between the regression models and the model test extrapolation. The brake power in the figure includes a sea margin of 15%. The service speed can be obtained for the corresponding normal continuous rating (NCR) power from the graph. The service speed differences between the proposed model and the model test are listed in Table 3. The absolute error of each model ranged from 0.7% to 3.0%. The overall shape of the power curve from the CNN model was the best among the present methods. The ratios of the integral of the absolute error of each method to the integral of the model test power curve for the corresponding speed range calculated using Equation (1) are listed in Table 4. The results confirmed that the CNN model presented the smaller error for the three cases. The error of the CNN model was larger than that of the MLP model in the case of the tanker; however, it was just 2.7%. The error in the shaft revolution speed at the NCR power without sea margin for all models was less than 7%.

Table 2. Main parameters of the tested ships.

		Bulk	**Container**	**LPGC**	**Tanker**
Hull	L (m)	176.00	206.55	165.00	320.00
	B (m)	30.0	30.6	28.0	60.0
	T (m)	9.5	10.2	10.4	21.0
	L_{CB} (%)	+2.4	−1.5	+0.75	+3.5
	C_B (-)	0.798	0.650	0.75	0.825
	Scale ratio (-)	24.4	30.0	26.0	39.6
	L_{bulb} (m)	4.3	6.2	5.7	6.5
	S_{BH} (m^2)	7362.1	8165.0	6750.7	28,873.0
	A_T (m^2)	574.4	900.4	524.8	1200.0
Propeller	D_P (m)	6.1	7.5	6.5	9.9
	Z (-)	4	5	4	4
	a_E (-)	0.486	0.710	0.525	0.485
	$p_{0.7R}$ (-)	0.768	0.971	0.897	0.743
	p_{mean} (-)	0.755	0.943	0.850	0.727

Table 3. Absolute error in the service speed.

Model	**Bulk**	**Container**	**LPGC**	**Tanker**
MLP	1.43%	1.38%	2.97%	0.31%
CNN	0.64%	0.69%	0.71%	1.12%
Exp	14.02 kts.	21.71 kts.	16.82 kts.	16.11 kts.

Table 4. Power prediction errors for each model.

Model	**Bulk**	**Container**	**LPGC**	**Tanker**
MLP	5.5%	4.9%	9.3%	1.2%
CNN	3.5%	1.9%	2.6%	2.7%

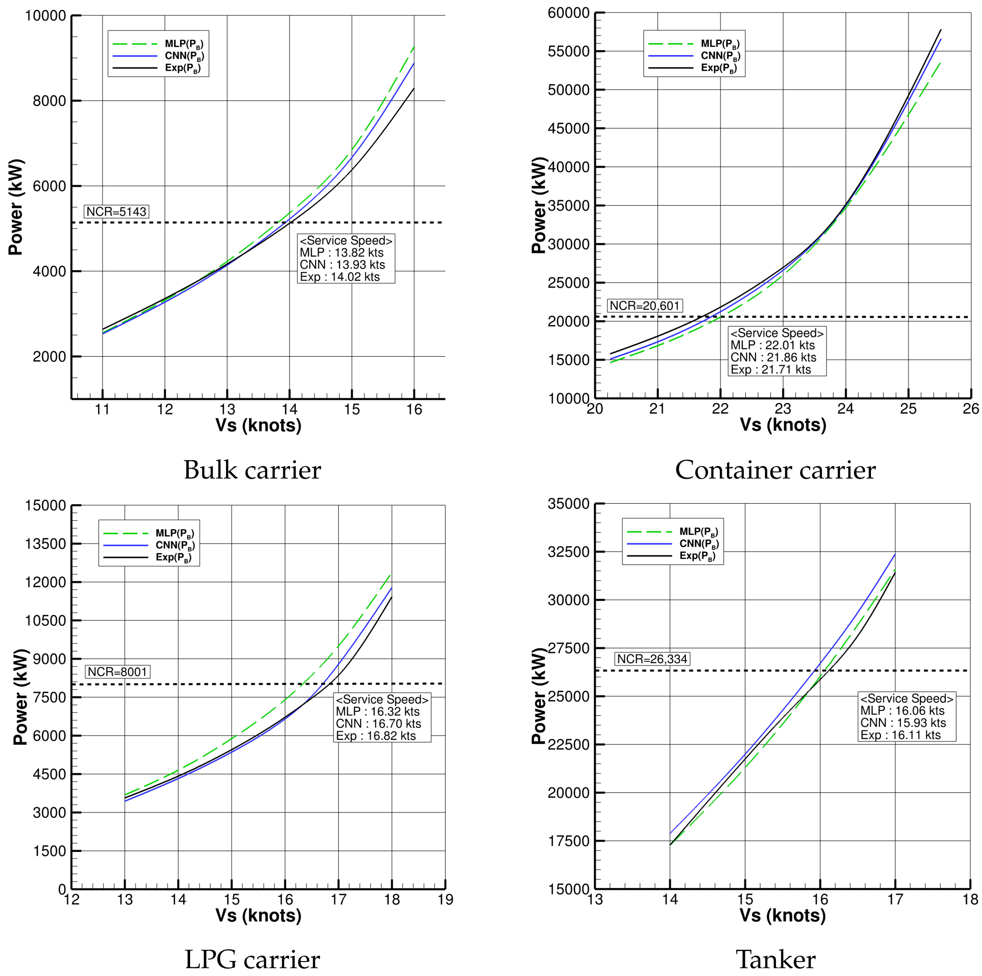

Figure 16. Power prediction results.

5. Concluding Remarks

This study introduced a power prediction method using regression models. In particular, regression models for the resistance, propulsion, and POW characteristics were obtained using an ANN. The model test results from the KRISO towing tank were used in the learning process. To consider the hull geometry, an image-based hull form representation method was suggested. The findings of this study can be summarized as follows:

- Development of MLP models for C_R, w_{TM}, and t
- Development of CNN models for C_R, w_{TM}, and t
  - Image-based hull form representation using a signed distance function
- Development of MLP models for K_{TM} and K_{QM}
- Development of power prediction method using the developed regression models

The results for C_R and w_{TM} showed good agreement with the model test; however, the estimated t was relatively poor compared with the other coefficients. Additional input variables related to the propeller performance, such as $p_{0.7R}$, might be required. The results confirmed that a simple MLP model can estimate the POW characteristics accurately. The CNN model showed less than a 1.5% difference in service speed from the model test extrapolation for the four selected hull forms in the test dataset. The trend of the CNN model was closest to the power curve shape of the experimental value. As expected, the MLP model showed less accuracy than the CNN model; however, this model can be used when the details of the hull geometry are unknown. The relatively low accuracy in the high-speed regions may be due to insufficient data around these regions, as shown in Figure 9.

The methods presented in this paper are feasible for the preliminary design stage. In particular, the CNN model can rapidly reduce the number of design alternatives for the optimal hull form design before using CFD because this model can capture the changing pattern of the cross-sections. However, data-driven prediction models, such as the present models, should be used with caution when applied to a completely new hull shape not included in the data used for learning. Furthermore, securing more model test data for improving the estimation models and nominal wakefield estimation using the present CNN approach will be part of future research work.

Author Contributions: Conceptualization, Y.-C.K.; methodology, Y.-C.K., G.-D.K. and K.-S.K.; software, Y.-C.K. and S.Y.; validation, Y.-C.K., G.-D.K. and Y.-Y.L.; formal analysis, Y.-C.K.; investigation, Y.-C.K. and M.K.; resources, Y.-C.K., G.-D.K. and M.K.; data curation, Y.-C.K., Y.-Y.L. and M.K.; writing—original draft preparation, Y.-C.K.; writing—review and editing, Y.-C.K. and K.-S.K.; visualization, Y.-C.K.; supervision, Y.-C.K.; project administration, Y.-C.K. All authors have read and agreed to the published version of the manuscript.

Funding: This research was supported by a grant from the Korea Research Institute of Ships and Ocean Engineering Endowment Projects funded by the Ministry of Oceans and Fisheries (1525014865, PES4731 and 1525014879, PES4872).

Institutional Review Board Statement: Not applicable.

Informed Consent Statement: Not applicable.

Data Availability Statement: Not applicable.

Conflicts of Interest: The authors declare no conflict of interest.

Nomenclature

The following abbreviations are used in this manuscript:

L	L indicates L_{PP} (Length between perpendiculars)
B	Breadth
T	Draught
C_B	Block coefficient
C_{BA}	Block coefficient of after body
L_{CB}	Longitudinal center of buoyancy
∇	Displacement volume
L_{bulb}	Bulbous bow length
D_P	Propeller diameter
Z	Number of propeller blades
a_E	Expanded blade area ratio
$p_{0.7R}$	Pitch ratio at 0.7R
p_{mean}	Mean pitch ratio
S_{BH}	Wetted surface area of bare hull
S_{BK}	Bilge keel area
A_T	Projected area of ship above the water line to the transverse plane
ρ_A	Mass density of air
ρ_W	Mass density of water
Fr	Froude number
Rn	Reynolds number
J	Propeller advance ratio
C_R	Residuary resistance coefficient
w_T	Wake fraction
t	Thrust deduction fraction
K_T	Thrust coefficient
K_Q	Torque coefficient
R_T	Total resistance

C_T	Total resistance coefficient
C_F	Frictional resistance coefficient
C_A	Incremental resistance coefficient for model ship correlation
C_{AA}	Air or wind resistance coefficient
P_B	Brake power
η_R	Relative rotative efficiency
η_T	Transmission efficiency
n	Propeller frequency of revolution
Symbols for subscript	M: model, S: ship

References

1. Taylor, D.W. *Speed and Power of Ships*; Press of Ransdell: Washington, DC, USA, 1933.
2. Gertler, M. *A Reanalysis of the Original Test Data for the Taylor Standard Series*; Navy Department the David W. Taylor Model Basin, Report 806; US Government Printing Office: Washington, DC, USA, 1954.
3. Lap, A.J.W. Resistance (Fundamentals of ship resistance and propulsion). *Int. Shipbuild. Prog.* **1956**, *3*, 441. [CrossRef]
4. Guldhammer, H.E.; Harvald, S.A. *Ship Resistances Effect of Form and Principal Dimensions*; Akademisk, Forlag: Copenhagen, Denmark, 1965.
5. Holtrop, J.; Mennen, G.G.J. A statistical power prediction method. *Int. Shipbuild. Prog.* **1978**, *25*, 253. [CrossRef]
6. Holtrop, J.; Mennen, G.G.J. An approximate power prediction method. *Int. Shipbuild. Prog.* **1982**, *29*, 166–170. [CrossRef]
7. Holtrop, J. A statistical re-analysis of resistance and propulsion data. *Int. Shipbuild. Prog.* **1984**, *31*, 272–276.
8. Kim, Y.C.; Kim, M.S.; Yang, K.K.; Lee, Y.Y.; Yim, G.T.; Kim, J.; Hwang, S.H.; Kim, K.S. Prediction of residual resistance coefficient of low-speed full ships using hull form variables and model test results. *J. Soc. Nav. Arch. Korea* **2019**, *56*, 448–457.
9. Kim, Y.C.; Yang, K.K.; Kim, M.S.; Lee, Y.Y.; Kim, K.S. Prediction of residual resistance coefficient of low-speed full ships using hull form variables and machine learning approaches. *J. Soc. Nav. Arch. Korea* **2020**, *57*, 311–321.
10. Cho, Y.I.; Oh, M.J.; Seok, Y.S.; Lee, S.J.; Roh, M.I. Resistance estimation of a ship in the initial hull design using deep learning. *Korean J. Comput. Des. Eng.* **2019**, *24*, 203–210. [CrossRef]
11. Bertram, V.; Mesbahi, E. Estimating resistance and power of fast monohulls employing artificial neural nets. In Proceedings of the International Conference High Performance Marine Vehicles, Rome, Italy, 27–29 September 2004.
12. Couser, P.; Mason, A.; Mason, G.; Smith, C.R.; von Konsky, B.R. Artificial neural networks for hull resistance prediction. In Proceedings of the Compit 2004, Siguenza, Spain, 9–12 May 2004.
13. Yang, Y.; Tu, H.; Song, L.; Chen, L.; Xie, D.; Sun, J. Research on accurate prediction of the container ship resistance by RBFNN and other machine learning algorithms. *J. Mar. Sci. Eng.* **2021**, *9*, 376. [CrossRef]
14. Cepowski, T. The prediction of ship added resistance at the preliminary design stage by the use of an artificial neural network. *Ocean Eng.* **2020**, *195*, 106657. [CrossRef]
15. Liu, S.; Papanikolaou, A. Fast approach to the estimation of the added resistance of ships in head waves. *Ocean Eng.* **2016**, *112*, 211–225. [CrossRef]
16. Liu, S.; Papanikolaou, A. Regression analysis of experimental data for added resistance in waves of arbitrary heading and development of a semi-empirical formula. *Ocean Eng.* **2020**, *206*, 107357. [CrossRef]
17. Liu, S.; Papanikolaou, A. Improvement of the prediction of the added resistance in waves of ships with extreme main dimensional ratios through numerical experiments. *Ocean Eng.* **2023**, *273*, 113963. [CrossRef]
18. Martić, I.; Degiuli, N.; Majetić, D.; Farkas, A. Artificial neural network model for the evaluation of added resistance of container ships in head waves. *J. Mar. Sci. Eng.* **2021**, *9*, 826. [CrossRef]
19. Martić, I.; Degiuli, N.; Grlj, C.G. Prediction of added resistance of container ships in regular head waves using an artificial neural network. *J. Mar. Sci. Eng.* **2023**, *11*, 1293. [CrossRef]
20. Yidiz, B. Prediction of residual resistance of a trimaran vessel by using an artificial neural network. *Brodogradnja* **2022**, *73*, 127–140. [CrossRef]
21. Ichinose, Y.; Taniguchi, T. A curved surface representation method for convolutional neural network of wake field prediction. *J. Mar. Sci. Technol.* **2022**, *27*, 637–647. [CrossRef]
22. Zhang, S. Research on the deep learning technology in the hull form optimization problem. *J. Mar. Sci. Eng.* **2022**, *10*, 1735. [CrossRef]
23. Scholcz, T.; van Daalen, E. Surrogate-based multi-objective optimisation for powering and seakeeping. In *Practical Design of Ships and Other Floating Structures*; Springer: Singapore, 2021; pp. 477–492.
24. Guerrero, J.; Cominetti, A.; Pralits, J.; Villa, D. Surrogate-based optimization using an open-source framework: The bulbous bow shape optimization case. *Math. Comput. Appl.* **2018**, *23*, 0060. [CrossRef]
25. Bresenham, J.E. Algorithm for computer control of a digital plotter. *IBM Syst. J.* **1965**, *4*, 25–30. [CrossRef]
26. Guo, X.; Li, W.; Iorio, F. Convolutional neural networks for steady flow approximation. In Proceedings of the 22nd ACM SIGKDD International Conference on Knowledge Discovery and Data Mining, San Francisco, CA, USA, 13–17 August 2016.
27. He, K.; Zhang, X.; Ren, S.; Sun, J. Delving Deep into Rectifiers: Surpassing Human-Level Performance on ImageNet Classification. *arXiv* **2015**, arXiv:1502.01852.

28. Ruder, S. An overview of gradient descent optimization algorithms. *arXiv* **2016**, arXiv:1609.04747.
29. Frazer, P.I. A tutorial on Bayesian optimization. *arXiv* **2018**, arXiv:1807.02811.
30. Degiuli, N.; Martić, I.; Farkas, A.; Buča, M.P.; Dejhalla, R.; Grlj, C.G. Experimental assessment of the hydrodynamic characteristic of a bulk carrier in off-design conditions. *Ocean Eng.* **2023**, *280*, 114936. [CrossRef]